RECHARGEABILITY AND RATE CAPABILITY OF POLYMER ELECTROLYTE BATTERIES AT ROOM TEMPERATURE

R. KOKSBANG*, I. I. OLSEN, P. E. TØNDER, N. KNUDSEN, J. S. LUNDSGAARD and S. YDE-ANDERSEN

Energy Research Laboratory A/S (ERL), Vestergade 24, DK-5700 Svendborg (Denmark)

Summary

The room temperature performance of rechargeable lithium batteries based on a novel polymer electrolyte is presented. The polymer electrolyte conductivity exceeds 1 mS/cm in the temperature range −40 to 60 °C and the mass transport properties are similar to those of non-aqueous liquid electrolytes. High materials utilisation is achieved at rates between $C/10$ and $C/1$. The rechargeability is similar to results obtained with liquid electrolytes and with high temperature, polymer-electrolyte-based batteries. During one minute pulses to 1.8 V, the peak power is approximately 20 mW/cm^2.

Introduction

Looking at, and beyond, the present battery markets, it is clear that a new type of advanced secondary battery is needed. A battery to suit future needs must meet some essential requirements, among which the most important are: high energy density, high power density, low cost, safety, long life and reliability. Several different types of advanced battery systems have been evaluated worldwide, with regard to these requirements. These systems include aqueous electrolyte batteries (Zn/air, Ni/Zn, Zn/Br$_2$, Al/air), organic and inorganic non-aqueous, liquid-electrolyte lithium batteries (Li/TiS$_2$, Li/SO$_2$), fused salt electrolyte batteries (Li/FeS$_2$) and solid electrolyte, alkali metal batteries (Na/S, Li/glass electrolyte/TiS$_2$, Li/(PEO)$_x$LiX/V$_6$O$_{13}$).

In these assessments the thick film, all solid state, lithium polymer electrolyte battery was found to best fulfil a majority of the requirements for the battery of the future; especially because this battery can be mass produced by modern coating and laminating technology. It provides high energy density combined with the possibility of high power because of the thin film concept. The laminate technology provides genuine design freedom

---

*Author to whom correspondence should be addressed.

in creating large area battery configurations. Batteries can be constructed in prismatic and cylindrical, as well as irregularly shaped configurations, in which the laminate is stacked, rolled, or folded, to match the shape of the encapsulation. The difficulties in realising a bipolar configuration with liquid-electrolyte-based systems are eliminated by the use of a flexible and mechanically stable solid-polymer electrolyte.

Furthermore, this battery has the possibility of a lifetime similar to that of the device for which it is intended. Future battery driven devices may therefore not have a battery container with exchangeable batteries, but batteries as integrated electronic components.

However, the low room-temperature ionic conductivity of conventional polymer electrolytes [1] limits the applications to those of very low power requirements, excluding batteries, electrochromics, etc., except for applications where higher temperatures are tolerable.

Since the first results on PEO-based systems were published in 1978 [2], significant improvements in room temperature performance have taken place, notably during the MHB collaboration between ERL and Mead Imaging, U.S.A. [3], in the ACEP collaboration between Hydro-Quebec in Canada and Elf and Laboratoire d'Electrochimique in France [4, 5] and at Harwell, U.K. [6]. Recently [3], we presented a novel polymer electrolyte with high conductivity (0.5 - 5 mS/cm) in a wide temperature range: —40 to
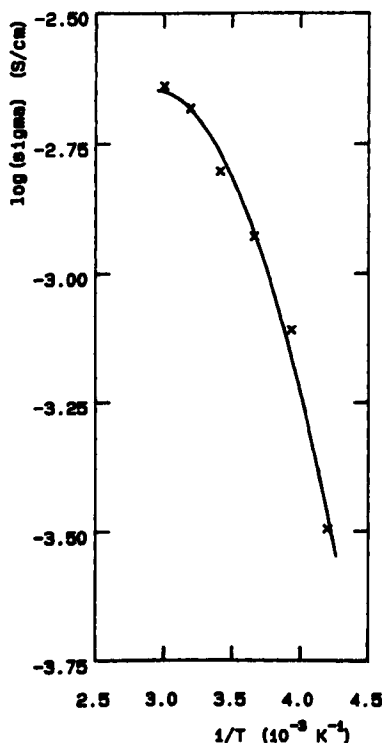

Fig. 1. Polymer electrolyte conductivity dependence on reciprocal temperature.

60 °C (Fig. 1). Excellent transport properties of the electrolyte were also demonstrated. The transference number of the lithium ion is approximately 0.5 and the salt diffusion coefficient is greater than 10^{-5} cm^2/s at room temperature. Thus, the polymer electrolyte has electrochemical properties similar to those of non-aqueous liquid electrolytes.

In this paper we present rechargeability data comparable with those obtainable with non-aqueous, liquid-electrolyte-based batteries and demonstrate that high rate discharge and high peak power are possible at room temperature using the electrolyte developed during the ERL/Mead Imaging collaboration.

Experimental

The laminate configuration is shown in Fig. 2, and consists of a lithium foil anode, a polymer electrolyte film and a composite cathode (1 - 3 mA h/cm^2) on a current collector. The latter could be a metal foil, *e.g.*, nickel as shown in the Figure, while the composite cathode consists of an intimate mixture of polymer electrolyte, acetylene black and V_6O_{13}. Other active cathode materials have been investigated but the results presented here will be restricted to V_6O_{13}-based batteries.

A typical test battery design is also shown in Fig. 2. Metal current collectors are attached to the laminate electrodes and the laminate is placed in a flexible encapsulation which is evacuated and heat sealed for protection of the battery laminate. This design provides easy access to different battery configurations, as it is easy to manufacture batteries as both single cells and as bipolar cells having higher voltage and with areas in the range from one to a few hundred cm^2.

In the following discussion the utilisation of the active cathode material is relative to eight moles of Li per mole of V_6O_{13}, which is the maximum reversible capacity [7 - 9] of the Li/V_6O_{13} couple. The estimation of the

EXTERNAL
CURRENT
COLLECTORS

15 Micron — CURRENT COLLECTOR
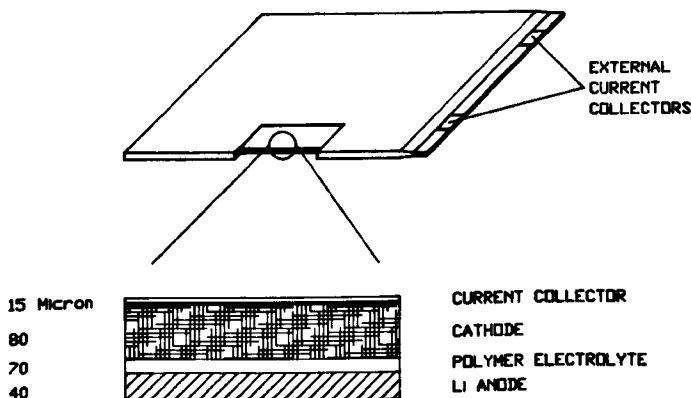80 — CATHODE
70 — POLYMER ELECTROLYTE
40 — LI ANODE

Fig. 2. Basic laminate and test battery design.

utilisation is based on the charge passed through the batteries and a chemical analysis of the vanadium content of the cathodes. Liquid electrolyte cells were assembled as previously described [10], by clamping 16 cm^2 cells between glass plates. Celgard 2400 poly(propylene) separators soaked in a 1 M LiCF$_3$SO$_3$/propylene carbonate solution were used and the cells were placed in O-ring sealed, flooded pyrex containers.

Cycling of batteries was realised using a personal-computer-based data acquisition system developed at the Energy Research Laboratory. The batteries were discharged to 1.8 V and recharged similarly to 3.0 V galvanostatically. To compensate for the *IR* drop, constant voltage charge for 1 - 2 h was applied after galvanostatic charging.

The peak power capabilities were determined by chronoamperometric techniques using a Solartron 1286 Electrochemical Interface controlled by a personal computer. A 1.8 V potential was applied to the cells and the current characteristic recorded as a function of time. The pulse duration was 1 min and the pauses between the pulses were 5 min.

Results and discussion

The voltage *versus* time curves at room temperature and at various cycle numbers, shown in Fig. 3, illustrate the discharge and charge behaviour of typical batteries. At the *C*/10 rate, full utilisation of the active cathode material is achieved in the first discharge. The number of plateaux, their relative sizes and voltage levels are identical to the *OCV* curve [7, 9] and show that the battery is close to equilibrium and that the overvoltage is negligible in both charge and discharge. Moreover, the voltage characteristics are identical to those observed in liquid electrolyte cells [7 - 9] at room temperature, as seen by comparison with Fig. 4. A similar agreement is evident by comparison with cells discharged at elevated temperature using conventional polymer electrolytes (9, 11). Even after 100 cycles the characteristic plateaux associated with the Li/V$_6$O$_{13}$ system can be distinguished (Fig. 3), also consistent with results obtained with liquid electrolytes (Fig. 4). The virtually unchanged shape of the voltage curves indicates that the integrity of the composite cathode is preserved and that no appreciable degradation of the vanadium oxide has taken place.

A comparison of the voltage *versus* time curves for the first cycle at different rates is shown in Fig. 5. The curves illustrate the discharge and charge behaviour of a typical battery laminate at higher rates at room temperature. At the *C*/5 rate the same general comments as given for the *C*/10 rate apply. At higher rates (*C*/2.5 and *C*/1) the characteristic shape changes to smooth and featureless due to the lower utilisation of the active material. However, high initial utilisation is observed, *i.e.*, more than 70% of the theoretical capacity at *C*/2.5 and more than 50% at *C*/1.

The rechargeability characteristics at *C*/10, *C*/2.5 and *C*/1 rates are illustrated in Fig. 6. Even at the *C*/1 discharge rate, more than 50%
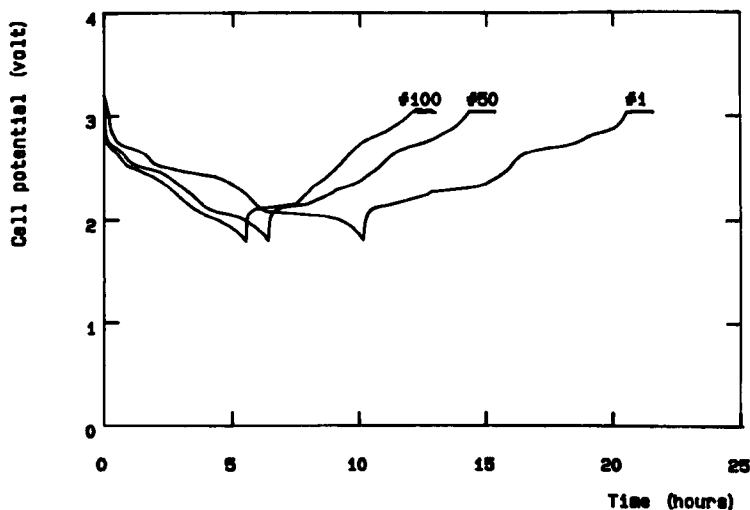
Fig. 3. Voltage characteristics at room temperature of polymer-electrolyte-based battery at a nominal $C/10$ rate: cycle nos. 1, 50 and 100.
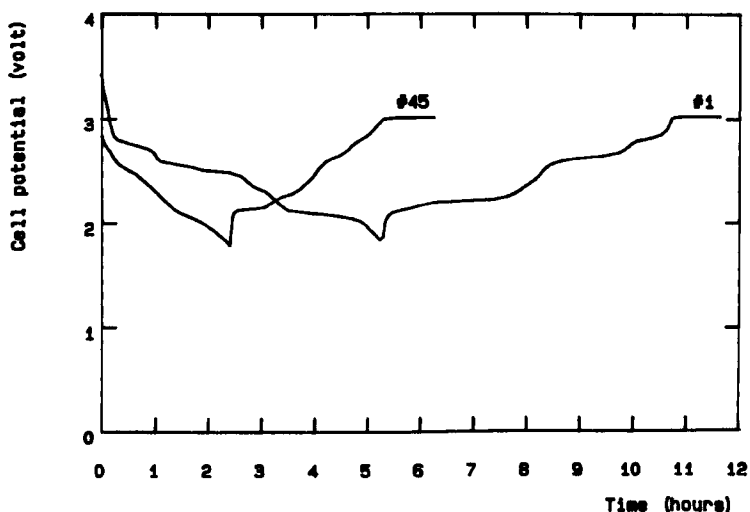

Fig. 4. Voltage characteristics at room temperature of liquid electrolyte (1 M LiCF$_3$SO$_3$/ PC) and V$_6$O$_{13}$ based batteries at a nominal $C/10$ rate: cycle nos. 1 and 45.

utilisation of the active material is apparent. The decaying capacity at low rate is similar to the performance observed with liquid electrolytes (Fig. 7). The decay at low rate is enhanced by insufficient recharge of the polymer battery, as the amount of charge used to recharge the battery is lower than the amount of charge extracted in the preceeding discharge. As the discharge and charge rates are identical, a better performance is to be expected by decreasing the charge rate, as is common with other batteries. This is supported by the observation that on decreasing the rates by a factor of ten,
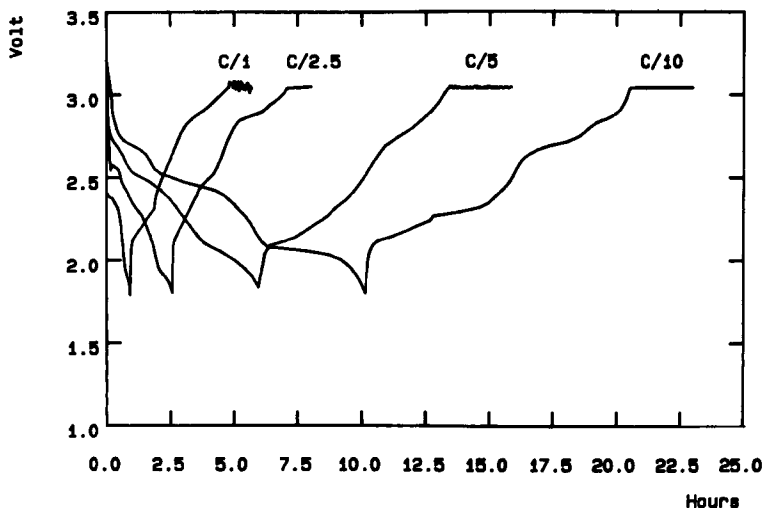
180

Fig. 5. Voltage *vs.* time curves for first cycle at room temperature at different rates of polymer-electrolyte-based batteries.
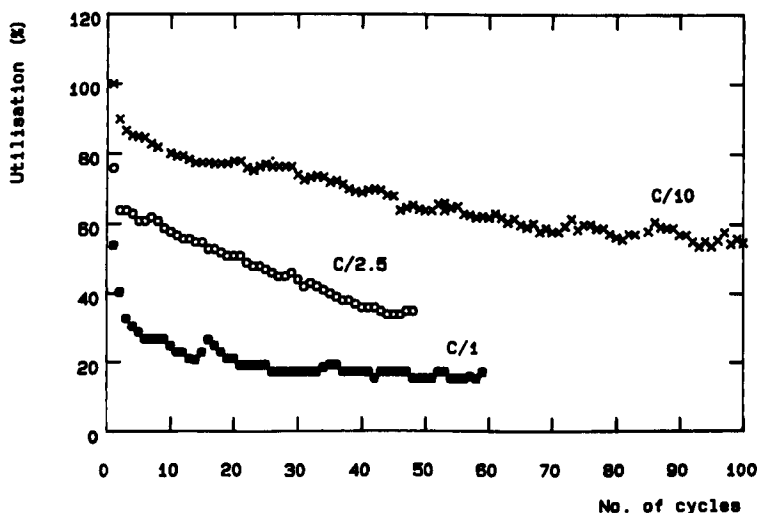

Fig. 6. Room temperature cycleability of polymer-electrolyte-based battery at the $C/10$, $C/2.5$ and $C/1$ rates. 100% utilisation corresponds to 8 Li/V$_6$O$_{13}$.

full utilisation is recovered. At the $C/2.5$ and $C/1$ discharge rates (Fig. 6), a faster decay of the capacity is observed, although the recharge rate is $C/5$ and $C/4$, respectively. The decaying capacity is presumably related to either increasing anode/electrolyte impedance or to the volume changes of the composite cathode due to lithium insertion in V$_6$O$_{13}$ [7 - 9, 11] which reduces the accessibility of inserted lithium in the cathode material.

In Table 1 the average utilisation of the cathode material is compared with that of both liquid-electrolyte cells and high temperature (PEO)$_9$-
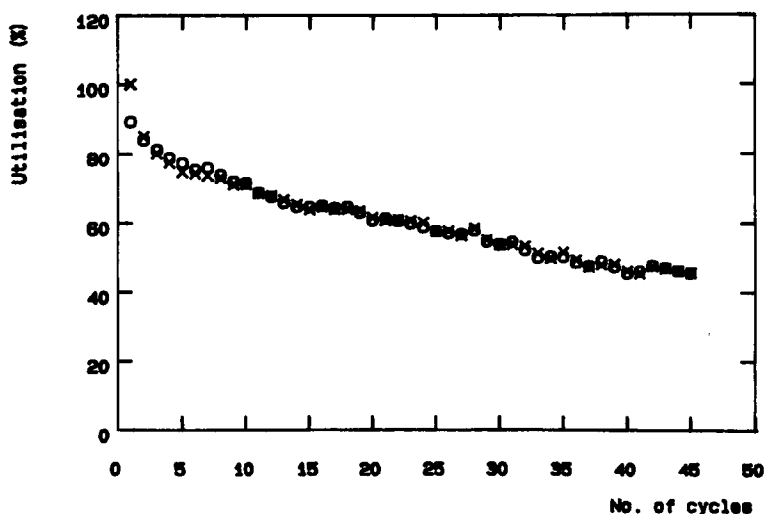
Fig. 7. Cycleability of liquid electrolyte cell at room temperature: x, discharge capacity; o, charge capacity. 100% utilisation corresponds to 8 Li/V_6O_{13}.

TABLE 1

Average cathode and anode utilisations. The 'Average Li/V_6O_{13}' and 'Utilisation of anode' are number of lithium inserted on average, and the number of times the total amount of lithium in the anode has been in use, respectively, during the cycle life indicated

Cell type	Average Li/V_6O_{13}	Utilisation of anode	No. of cycles	Reference
(PEO)$_9$LiCF$_3$SO$_3$	3.6	3	100	9
1 M LiAsF$_6$/PC	4.3		100	9
1 M LiCF$_3$SO$_3$/PC	5.6	1.6	45	this work
Polymer electrolyte				
C/10	5.4	2.2	100	this work
C/2.5	4.5	1.2	50	

LiCF$_3$SO$_3$-based cells. The comparison shows that our polymer-electrolyte-battery performance is identical to both liquid electrolyte and other polymer-electrolyte batteries. Similarly, the rechargeability of the anode appears to be as good as that of liquid electrolyte- and PEO-based cells, as seen in Table 1, as an amount of charge corresponding to more than twice the amount of the pristine lithium present has been plated.

Typical results of maximum current (initial and at the end of the one minute pulses), as well as the discharge capacity of individual pulses and the accumulated discharge capacity, are shown in Fig. 8, for a cell discharged potentiostatically to 1.8 V for 1 min. The maximum current density obtainable approaches 20 mA/cm^2 initially, decreasing to approximately 5 mA/cm^2 towards the end of the 1 min pulse. Not unexpected, the current
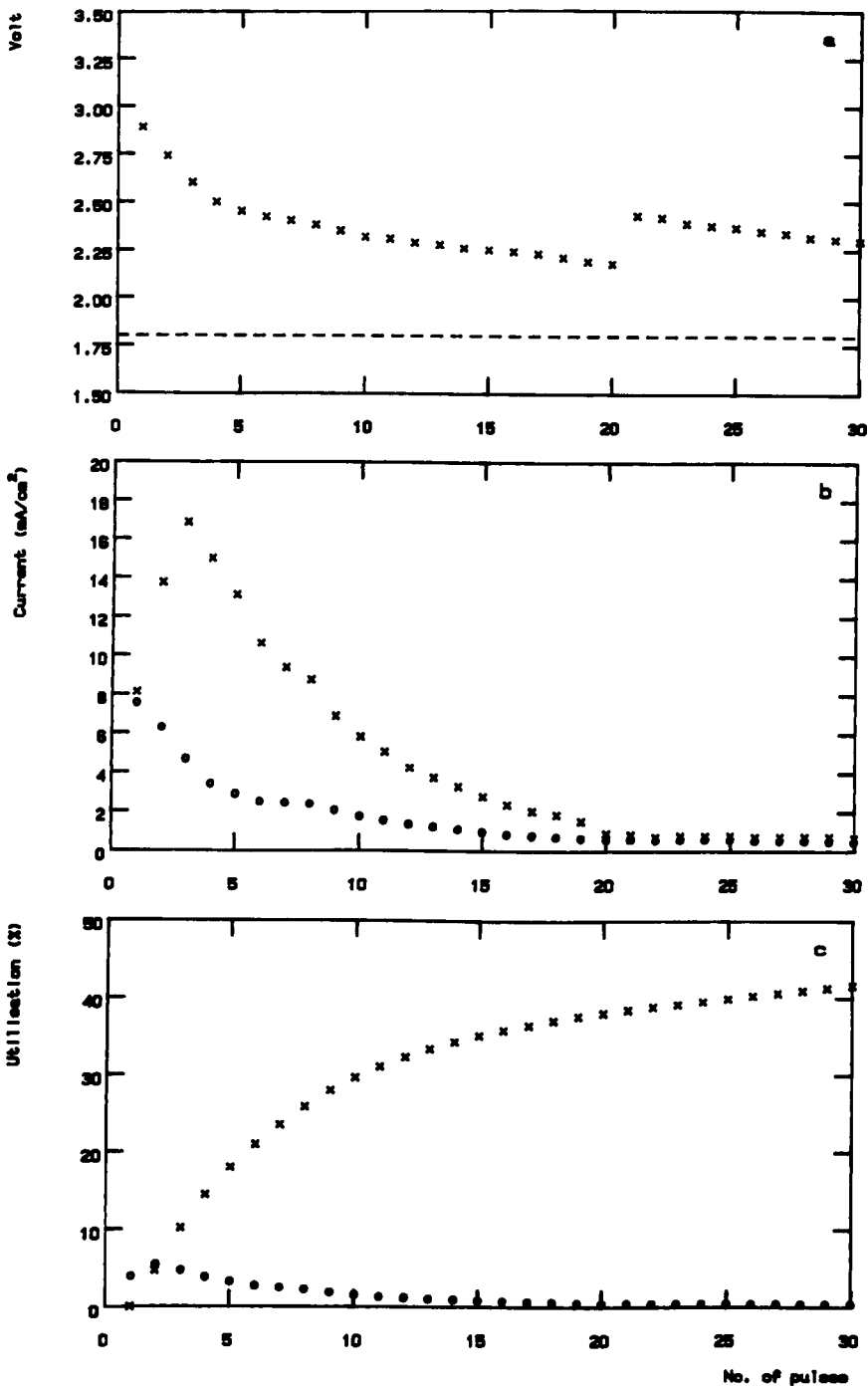
Fig. 8. Potentiostatic pulse discharge to 1.8 V at room temperature. (a) *OCV* (×) and discharge potential (— — —); (b) initial maximum (×) and minimum (after 1 min) (○) current densities; (c) utilisation (○) of the active material in each pulse and accumulated materials utilisation (×).

density decreases as a function of the number of pulses. The maximum utilisation of the cathode material is approximately 5% in the first pulse, decreasing in the following pulses, while the accumulated utilisation exceeds 40% during 30 pulses. The cell was allowed to rest at OCV for 15 h between pulses 20 and 21. No beneficial effect on the current density was observed after this rest period although the OCV increased from approximately 2.2 V to more than 2.45 V, presumably because of the decreasing electronic conductivity and lithium diffusion coefficient of V_6O_{13}, when the utilisation exceeds 50% of the theoretical capacity.

The average current density obtained during the first pulse at 1.8 V corresponds to an average peak power of approximately 20 mW/cm^2.

These results compare favorably with room temperature results recently released by Hooper et al. [6] for similar cells based on a polymer electrolyte developed at Harwell. High currents were observed in 12 s pulses. However, except for the first pulse, they observed very low capacities.

A common battery design is the cylindrical type which utilises the Swiss roll configuration. Table 2 summarises the battery laminate specifications calculated for three different battery sizes with the ANSI designations: AA, C and D, with the dimensions (diameter × height in mm) 14.5 × 50, 26 × 50 and 34 × 62, respectively. A capacity of 3 mA h/cm^2 laminate is assumed in the calculations, together with a simple design corresponding to the laminate configuration sketched in Fig. 2. The width of the laminate is 50 mm and the thickness is 215 μm, as given in Table 3. An electronically insulating layer of 10 μm is included to prevent short circuit of the battery.

The laminate capacities of the AA, C and D cells are 0.9, 3 and 5 A h, respectively. This gives a battery capacity of around 0.8 A h for the AA cell, 2.8 A h for the C cell and around 4.5 A h for the D cell when approximately

TABLE 2

Swiss roll battery types

	Battery type		
	AA	C	D
Volume (cm^3)	6.9	23.9	40.9
Laminate			
Volume (cm^3)	6.2	21.5	36.8
Length (cm)	57.5	200	315
Area (cm^2)	288	996	1704
Weight (g)	13.2	45.5	78.0
Capacity (A h)	0.9	3	5
Battery			
Capacity (A h)	0.8	2.8	4.5
Energy (W h)	1.9	6.7	10.8
Peak power (W)	5.8	20	34
Peak current (A)	5	15	25

TABLE 3

Battery laminate specification

Component	Thickness (μm)
Nickel foil	15
Cathode	80
Electrolyte	70
Lithium	40
Total	205
Insulating polymer foil	10

10% of the volume is assumed to be used for current collector connections, etc. The expected capacities thus exceed those of conventional Ni/Cd batteries and are comparable with, or better than, those of the rechargeable Li/MnO$_2$, MoliCell batteries (0.6 A h, 1.8 W h, AA cells).*

Obviously, the expected performance depicted in this paper is pessimistic, as both layer thicknesses and laminate configuration can be optimised to give higher volumetric and specific capacities. It is, for example, easy to decrease the electrolyte thickness to less than 50 μm, and utilise cell designs based on laminate configurations with double-sided coatings and thereby reduce the weight and volume of inactive components relative to the amounts of active components.

Conclusions

The high conductivity of the polymer electrolyte developed at ERL, together with the processes developed for film formation and lamination, ensure high utilisation of the active materials at room temperature, good rate capabilities and good charge retention during cycling, and current densities sufficient for commercialisation of the polymer-electrolyte battery.

Scaling of the results obtained with flat plate cells to AA, C and D size cylindrical cells, shows that these batteries compare favorably with already existing battery technologies. The battery components are similar to those in use for non-aqueous, liquid-electrolyte systems. The electrolyte contains no expensive raw materials and the battery laminate is manufactured by continuous coating processes, resulting in a production with low labour costs. The battery is therefore able to substitute the major secondary battery systems as well as primary alkaline battery systems, the latter by substitution of V$_6$O$_{13}$ with MnO$_2$.

---

*Molicell, New Product Data Sheet, AA size cells, model 06 X 600.

Acknowledgements

References

1 J. R. MacCallum and C. A. Vincent (eds.), *Polymer Electrolyte Reviews 1*, Elsevier Applied Science, London, U.K., 1987; *Polymer Electrolyte Reviews 2*, Elsevier Applied Science, London, U.K., 1989.
2 M. B. Armand, J. M. Chabagno and M. Duclot, *2nd Int. Meet. Solid Electrolytes, St. Andrews, Scotland, U.K., Sept. 20 - 22, 1978*, Ext. Abstr., in P. Vashishta, J. N. Mundy and G. K. Shenoy (eds.), *Fast Ion Transport in Solids*, North Holland, Amsterdam, 1979.
3 J. S. Lundsgaard, S. Yde-Andersen, R. Koksbang, D. R. Shackle, R. A. Austin and D. Fauteux, in B. Scrosati (ed.), *Proc. 2nd Int. Symp. Polymer Electrolytes, Siena, Italy, June 14 - 16, 1989*, Ext. Abstr.
4 M. Gauthier, D. Fauteux, G. Vassort, A. Belanger, M. Duval, P. Ricoux, J.-M. Gabano, D. Muller, P. Rigaud, M. B. Armand and D. Deroo, *J. Electrochem. Soc., 132* (1985) 1333 - 1340.
5 M. Armand, W. Gorecki and R. Andreani, *Proc. 2nd Int. Symp. Polymer Electrolytes, Siena, Italy, June 14 - 16, 1989*, Ext. Abstr.
6 A. Hooper, R. J. Powell, T. J. Marshall and R. J. Neat, *J. Power Sources, 27* (1989) 3 - 13.
7 D. W. Murphy, P. A. Christian, F. J. DiSalvo and J. N. Carides, *J. Electrochem. Soc., 126* (1979) 497 - 499.
8 K. M. Abraham, J. L. Goldman and M. D. Dempsey, *J. Electrochem. Soc., 128* (1981) 2493 - 2501.
9 K. West, B. Zachau-Christiansen, T. Jacobsen and S. Atlung, *J. Power Sources, 14* (1985) 235 - 245.
10 R. Koksbang, D. Fauteux, P. Norby and K. A. Nielsen, *J. Electrochem. Soc., 136* (1989) 598 - 605.
11 K. West. B. Zachau-Christiansen, M. J. L. Østergaard and T. Jacobsen, *J. Power Sources, 20* (1987) 165 - 172.